Heliyon 9 (2023) e21239

Contents lists available at ScienceDirect

Heliyon

journal homepage: www.cell.com/heliyon

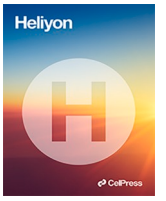

Multi-analytical investigation of the physical, chemical, morphological, tensile, and structural properties of Indian mulberry (*Morinda tinctoria*) bark fibers

Gurukarthik Babu Balachandran [a], P. Narayanasamy [b], Anandha Balaji Alexander [a], Prince Winston David [a], Rajesh Kannan Mariappan [a], Muthu Eshwaran Ramachandran [c], Suyambulingam Indran [d], Sanjay Mavinkere Rangappa [d,*], Suchart Siengchin [d]

[a] *Department of Electrical and Electronics Engineering, Kamaraj College of Engineering and Technology, Virudhunagar, 626001, Tamil Nadu, India*
[b] *Department of Mechanical Engineering, Kamaraj College of Engineering and Technology, Virudhunagar, 626001, Tamil Nadu, India*
[c] *Department of Computer Science and Engineering, Kamaraj College of Engineering and Technology, Virudhunagar, 626001, Tamil Nadu, India*
[d] *Natural Composites Research Group Lab, Department of Materials and Production Engineering, The Sirindhorn International Thai-German Graduate School of Engineering (TGGS), King Mongkut's University of Technology North Bangkok (KMUTNB), Bangkok, Thailand*

ARTICLE INFO

Keywords:
Morinda tinctoria fiber
Cellulose
Microfiber
Zeta potential
Structural characterization

ABSTRACT

In this study, micro-cellulosic fibers were isolated from the bark of *Morinda tinctoria* (MT) and characterized for the first time. The anatomical, physical, chemical, thermal, and mechanical properties of the *M. tinctoria* bark fiber (MTBF) were investigated. The mean diameter and density values were determined to be 32.013 ± 1.43 μm and 1.4875 g/cm^3, respectively. Zeta potential analysis and particle size measurements provided the evidence of enhanced micro-particle behavior on the fiber's surface. Various structural characterizations confirmed the presence of polysaccharide structures, monosaccharide compositions, glycosidic residues (sugar linkages), and cohesive reactions of TMSA (Trimethylsilyl alditol) derivatives, indicating the fiber's potential for strong surface absorption properties. X-ray diffraction analysis revealed a crystallinity index of 51 % and a crystallite size of 3.086 nm for MTBF. Fourier transform infrared analysis indicated the presence of cellulose, hemicellulose, and lignin constituents, along with their corresponding functional groups. The calculated values of Young's modulus and tensile strength were determined to be 75.7 GPa and 746.77 MPa, respectively. Thermogravimetric analysis demonstrated the thermal stability of the extracted MTBF up to 240 °C. Based on these findings, the MT microfibrils derived from the bark can be considered as potential substitutes for existing synthetic composites, offering reinforcement for novel bio composites.

1. Introduction

Over the last few decades, concepts based on sustainability, ecology, and green manufacturing steered to the generation of new bio-based polymer composite materials [1]. Requirement for green polymer cellulosic bio-composites based on bark fibers have a great

* Corresponding author.
E-mail address: mavinkere.r.s@op.kmutnb.ac.th (S. Mavinkere Rangappa).

https://doi.org/10.1016/j.heliyon.2023.e21239
Received 10 April 2023; Received in revised form 5 October 2023; Accepted 18 October 2023
Available online 27 October 2023
2405-8440/© 2023 Published by Elsevier Ltd. This is an open access article under the CC BY-NC-ND license (http://creativecommons.org/licenses/by-nc-nd/4.0/).

scope in the research areas like dielectric applications [2,3]. In recent days ligno-cellulosic fibers are available in large quantities. They are extracted from various plants because they are lightweight, biodegradable, environmentally friendly, and more suitable for reinforcements in polymer composites [4]. It is very significant and sustainable to get a source of reproducible high cellulosic fiber [5].

Natural fibers are nothing but micro-fibrils like MTBF imbibed with cellulose, matrix of non-cellulosic components like crystalline hemi-cellulose & lignin [6]. The cellulosic fibers were extracted and its characterization studies were carried out from different plant parts such as bark [7], stem [8], pod [9], blossom pedal [10], vegetables [11], fruit [12], fruit bunch [13], nutshell [14], leaf [15], and root [16]. They can be used as natural reinforcement or filler materials in polymer composites. They have wide applications in various industries such as packaging, automotive, aerospace, ship construction, and building materials production. The selection of cellulosic fiber as an organic filler is a better reinforcement for polymer composite materials [1]. Handicraft industries also prefer to use extracts of bark fibers due to their owing properties of lightness, high durability and elastic flexibility [17].

Morinda tinctoria (MT), commonly known as Indian mulberry, is a species of flowering plant belonging to the family *Rubiaceae*, which is native to South Asia. The plant is extensively cultivated in India to make morindone dye. Plant dyes have been widely used for coloring and other purposes [18]. The coloring substance named morindone is found in the root bark of MT and is collected when plants reach 3–4 years of age. Morindone is used for dyeing cotton, silk, and wool in shades of red, chocolate, or purple.

Earlier researches in this genus *Morinda* were listed in this segment. The dye fraction obtained from the methanolic extract of the roots of MT was explored for its role in attenuating damages caused by H_2O_2-induced oxidative stress [18]. The feasibility of using a low-cost biomass-based activated carbon from the bark of MT coated with Aluminium hydroxide for water de-fluoridation at the neutral pH range was studied [19]. MT leaf extract was used for corrosion inhibition in Aluminium and copper in an acid medium [20,21]. The different extract of MT leaves contain a broad spectrum of secondary metabolites and exhibit substantial antimicrobial activity against all the tested microorganisms. MT plant can be used to discover bioactive natural products that may lead to the development of new pharmaceuticals [22]. Natural compounds, namely iridoid glycoside and tinctoroid, are extracted from the roots of a prominent dye-yielding plant named MT (Linn.) Roxb. These compounds are endowed with rigorous bioactivities, which may be

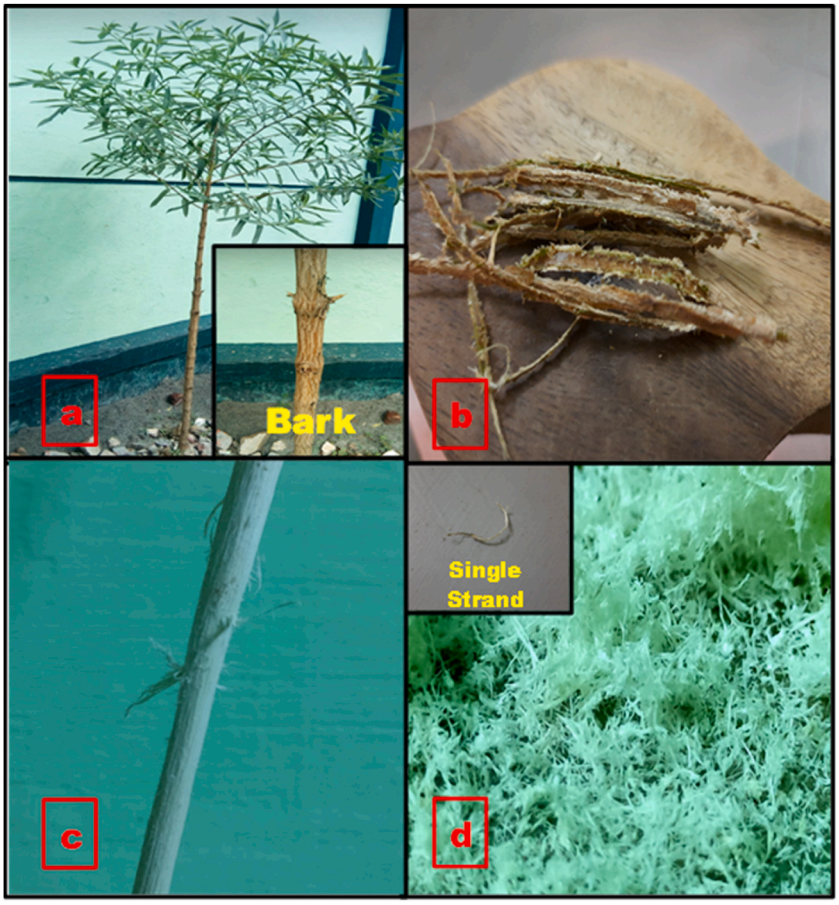

Fig. 1. *Morinda tinctoria* fiber extraction process
a) MT plant
b) Unruffled bark fibers
c) Unruffled bark
d) Unruffled MT microfibrils.

useful in drug discovery [23]. Silver nanoparticles were synthesized using acetone leaf extracts of MT. The larvicidal potential ability was tested against third instar larvae of *Culex quinquefasciatus.* The aqueous silver ions can be reduced by aqueous extract of MT plant parts to prepare very stable silver nanoparticles in water [24]. Furthermore, hepatoprotective effect of MT leaves has been studied and reported. The hepatoprotective activity of plant extracts was investigated for paracetamol-induced hepatotoxicity in rats [25]. All the research works are evident that our extent of work in characterizing the MTBF is novel and innovative towards making it a green bio-composite.

The MT plant is a fibrous plant that could be used for numerous domestic and medical purposes [24,25]. MT plants are grown for firewood and have rich fiber content in the bark as well as in the stem. Bark fibers from natural plants are suitable for filler/-reinforcement materials to fabricate polymeric composites ([7,26,27]) because they are stable in different climatic conditions.

No reports were available on the characterization, properties and uses of natural cellulose fibers from the bark of MT plant. Hence, an approach was developed for extraction and characterization of bark fibers from the MT plant as an environment-friendly biodegradable potential filler/reinforcement material for polymeric bio composites from bark fibers of MT plant [28]. The fiber can also be treated with alkalis in future works for its study on efficiency and change of behavior in aspects of all its physio-chemical and mechanical properties similar to earlier works like [29,30].

2. Materials and methods

2.1. Fiber extraction and preparation of microfibrils

A novel MT bark of 5 mm diameter was unruffled from a mature MT (Indian mulberry) plant at K. Vellakulam, Madurai District, Tamil Nadu, India, in the year 2019. It is shown in Fig. 1(c). The unruffled bark was cleaned with deionized water to remove dust and foreign particles. The fibers were peeled out by mechanical process. The fiber extracted was heated for 2 h at 70 °C to remove moisture [5,21].

The microfibrils were fibrillated from MTBF. The fibrillation process was done with the help of a Super mass colloider (model MKZA10 15J; Masuko Sangyo, Japan) [31]. The unruffled microfibrils are shown in Fig. 1(d).

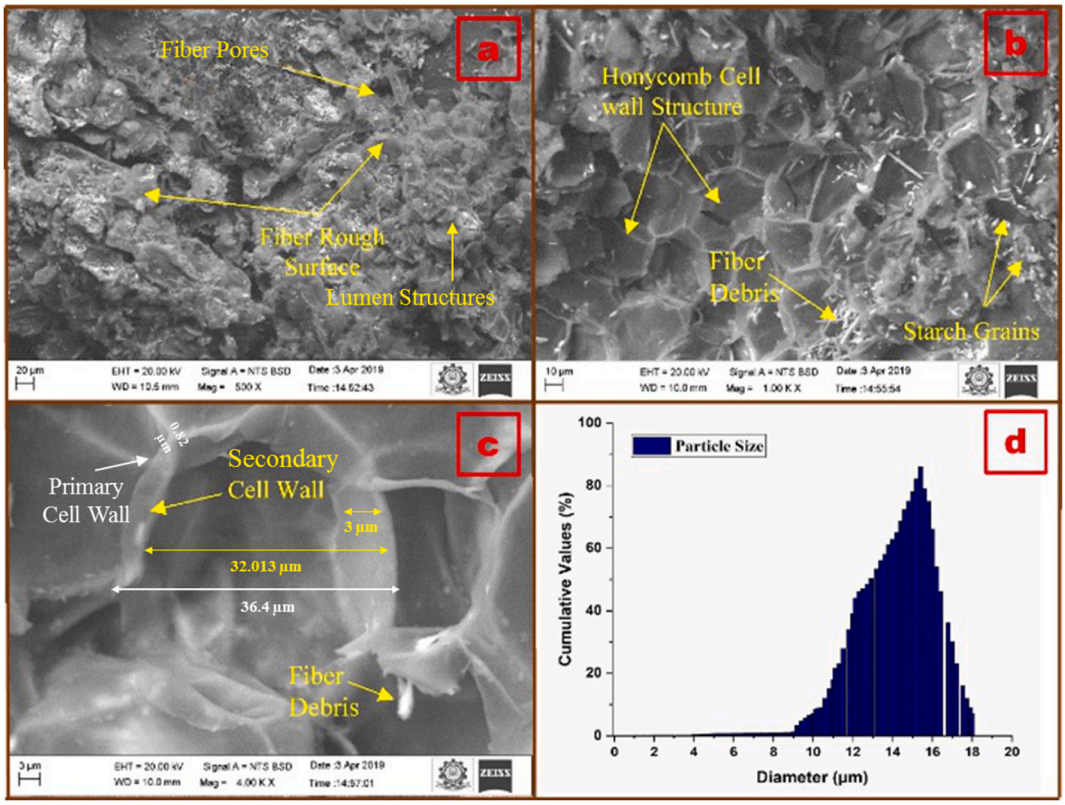

Fig. 2. SEM Analysis
a) 20 µm, transverse section
b) 10 µm, inner structure-low magnification
c) 3 µm, inner structure-high magnification
d) Particle size analysis.

2.2. Experimental characterization analysis

2.2.1. Bark anatomy and morphological analysis

Fig. 1(a–d) shows the fiber extraction process. The morphology of MT fiber was studied using scanning electron microscopy (SEM). The SEM analysis for MT fiber was carried out by using a Zeiss DSM scanning electron microscope (model 940A). Gold coating was done on the specimen using a K550 Emitech metalizer under argon atmosphere. The fibers were analyzed microscopically under 10–40 × magnification. The dimensions of the fiber were measured using SEM studies. The transversal view of the fiber was studied and captured [9]. Fig. 2(a–c) and 2(d) shows the SEM images and particle size distribution of MTBF respectively. The particle size of the fiber was measured by using a Zeta potential meter (MicroZS 3000; Malvern, Zetasizer) [32].

2.3. Physical analysis

For measuring the density of fiber, 2 g samples were subjected to an inert gas atmosphere at approximately 23 °C. This procedure was followed by powdering and drying in an air oven at approximately 56 °C for 2 h, as discussed in Ref. [9]. The density (ρ_{MTF}) of the bark fiber was evaluated by a pycnometer by using the equation given below [33]:

$$\rho_{MTF} = \rho_t \left({}^{(m_2 - m_1)}/_{(m_3 - m_1)(m_4 - m_2)} \right) \tag{1}$$

where ρ_{MTBF} – density of MTBF in g/ cm^3.
ρ_t – density of toluene in g/ cm^3.
m_1 – empty pycnometer mass in g
m_2 – chopped fiber-filled pycnometer mass in g
m_3 – toluene-filled pycnometer mass in g
m_4 – chopped fiber and toluene-filled pycnometer mass in g

2.4. Chemical analysis

Chemical analysis was conducted to characterize the percentage composition of cellulose, hemicellulose, lignin, wax, and moisture in the fiber sample. The amount of cellulose present in the MTBF was calculated by using Kurshner-Hoffer method [34], where the sample is powdered and made to react with dichloromethane. The resultant sample specimen was then treated with a solution of ethanol and 0.95 N nitric acid. The cellulose constituents remained insoluble after the experiment, which is separated and measured for cellulose content. Hemicellulose was quantified by using NFT 12-008 standards [9].

The amount of lignin present in the MTBF was calculated using the Klason method [35], in which the specimen is crushed and initially treated with dichloromethane. The resultant specimen was then hydrolyzed using 0.72 N of sulfuric acid. Lignin contents remained insoluble. The amount of unreacted lignin was measured to establish the lignin composition in the fiber sample.

The amount of wax present in the MTBF was calculated using the Conrad method [9], in which samples are initially crushed to powder and the extraction process is carried out for 6 h in a Soxhlet apparatus by using ethanol. Polysaccharides, wax and other alcohol soluble constituents remain unreacted. By the addition of chloroform, the Wax was separated from the unreacted residue and after evaporation of chloroform, the wax content was weighed to find the exact composition of wax in the MTBF.

The moisture content were calculated using the below equation [33]:

$$\%\ \text{Moisture} = \frac{Specimen\ weight\ (Before\ drying) - Specimen\ weight\ (After\ drying)}{Specimen\ weight\ (Before\ drying)} \times 100\ \% \tag{2}$$

2.5. Structural characterizations

2.5.1. Molecular weight determination

The molecular weights of the specimen were determined using size-exclusion chromatographic technique of gas chromatography mass spectrometry (GC/MS), as discussed earlier in Ref. [36]. A light scattering detector was used for molecular weight analysis using the high-performance size-exclusion chromatography–evaporative light scattering detector (HPSEC-ELSD) method. Dextran standards were used as calibration curves. The experimental procedure was carried out as follows: MTBF samples with dextran standards (5 mg each) were dissolved in 1 mL deionized water. The solution was tested on a 0.22-μm filter as per the HPSEC–ELSD analysis. The molecular weights were calculated using the calibrated equation (3) concerning Ref. [36]:

$$\log M_w = -0.67\ t_R + 8.21 \tag{3}$$

where M_w - molecular weight
t_R - retention time

2.6. Monosaccharide compositions

Monosaccharide compositions of MTBF were measured by using a GC/MS analyzer (model 7890A 5975C; Agilent) concerning [36]. The procedure was as follows: initially, the fiber sample was cleaned using methanol. Then 2 M trifluoroacetic acid (TFA) components were neutralized through evaporation by keeping them idle in a closed apparatus for some time at room temperature. The samples were then treated using trimethylsilyl alditol (TMSA). Specific monosaccharide constituents of MTBF were separated and quantified using the GC/MS analyzer.

2.7. Colorimetric method

Colorimetry was used to determine the presence of allied fiber components such as carbohydrates, uronic acid, proteins, sulfates, and acetyl polysaccharides as per the procedure stated in Ref. [36]. The phenol-sulfuric acid method was used to measure the composition of carbohydrates. The carbazole-sulfuric acid method was carried out to determine the composition of uronic acids in the bark fiber [37]. Furthermore, Coomassie blue protein technique was used to determine protein concentrations in the fiber sample. Sulfate constituents were detected using barium chloride–gelatin method on the fiber specimen. The hydroxylamine colorimeter test was performed to identify the presence of O-acetyl polysaccharides in the bark fibers.

2.8. Methylation

Methylation was carried out to find partially methylated alditol acetates and glycosidic (sugar) linkages as per the procedure stated in Ref. [36]. Various linkages of sugar components such as man (D-mannose), Ara (L-arabinose), Gal (D-galactose), and Rha (L-rhamnose) were identified along with their linkage patterns using the GC/MS method. The existence of sugar linkages in bark fibers confirmed the existence of monosaccharaides in MTBF constituents. The coexistence of monosaccharaide compositions were earlier found in *Aralia elata* root barks [36], which describes its structural behavior under critical temperature.

2.9. Smith degradations

Smith degradation procedure was performed to estimate the reactivity of TMSA derivatives. The procedure was as follows: first, 30 mg fiber specimens were taken for analysis by dissolving them in a solution of 30 mM NaI O_4 and distilled water. The specimens were tested using a spectrophotometer to analyze both Smith degraded elements and monosaccharaides. The procedure was repeated by treating fiber samples with acetic acid, NaB H_4, and 2 M TFA. A similar experiment was carried out earlier in Ref. [36]. Table 1 denotes the supplier details of chemicals and reagents procured for performing structural characterization.

2.10. XRD and FTIR analyses

The XRD analysis was performed using a Bruker Eco D8 advance diffractometer system [9] (Cu-Kα radiation) for the wavelength of 1.54 Å. The crystallite size (CS) and crystallinity index for MTBFs were calculated using the Scherer formula (equation (4)) and Segal equation (equation (5)), respectively.

$$L = \frac{k\lambda}{\beta \cos\theta} \tag{4}$$

where k – Scherer constant ($k = 0.89°$) [14]
λ – Wavelength of X-ray
β – full width peak
θ – Bragg angle

Table 1
Procurement of chemical and reagents [36].

Chemical/Reagent	Supplier
Dichloromethane	Sigma-Aldrich (St. Louis - USA)
Ethanol	
Nitric acid	
Sulfuric acid	
Chloroform	
Methanol	
Trimethylsilyl alditol (TMSA)	
$NaIO_4$	
$NaBH_4$	
Acetic acid	
Trifluoroacetic acid (TFA)	Merck, Zdarmstadt (Germany)
Distilled Water & Deionized Water	V V Enterprises, Madurai (Tamilnadu)

The Bragg peak values (at integrated intensities) help to calculate CI by using the Segal equation [33]:

$$\text{CI}\ \% = \frac{I_{CP} - I_{AP}}{I_{CP}} \times 100\ \% \tag{5}$$

where I_{CP} - intensity of crystalline peak

I_{Am} - intensity of amorphous peak

A Fourier transform infrared (FTIR) spectrometer (model FTIR-8400S Spectrum; Shimadzu, Japan) was used to study the functional groups present in the MTBF. FTIR analysis was performed with the lateral settings of 30 mA current and 40 kV Generator at 4 cm^{-1} resolution and in the range between 450 and 4000 cm^{-1} [13,38].

2.11. Thermal analysis

The thermal degradation of the MTBF was analyzed using Mettler Toledo TGA–SDTA at 500 °C in an inert atmosphere. The temperature variations and degradation evaluation were obtained from the Mettler STARe evaluation software for further analysis [39]. The KE (kinetic activation energy) was calculated using Broido's equation [40]:

$$\varepsilon = \ln\left(\ln\left(\frac{1}{Y}\right)\right) = -\left(\frac{E}{R}\right)\left(\left(\frac{1}{T}\right) + k\right) \tag{6}$$

where Y – Normalized weight (Q_t/Q_0),

Q_t Weight of sample at time t,

Q_0 Initial Sample weight,

E – Kinetic activation energy

R – Universal gas constant (R = 8.32 kJ/mol-K)

T – Temperature (K)

k – Reaction rate constant

2.12. Single fiber tensile test

The single-fiber tensile test was carried out on the MTBF to determine the various mechanical properties such as shearing strength and Young's modulus of the fiber specimen, regarding the ASTM standards (D 3322–01). Initially, the diameter of every fiber considered for the experiment purpose was measured at 3 alternative locations with the help of BMM (Binocular Motic Microscope, Model - Zeiss Axio Scope A1, Germany). A total of 30 trial experiments were conducted for different single strands of fibers tested at 2.5 mm/min cross head speed. The tensile test experiment was carried out with the help of a ZwickRoell machine (2.5 kN load cell) [41]. The interfacial shear strength (τ_d) of the sample was calculated using the equation as stated below [42]:

$$\tau_d = \frac{F_{max}}{\pi d l_e} \tag{7}$$

where F_{max} - Maximum force

d- diameter of the fiber

l_e - Effective length of fiber

The Young's modulus value was calculated from the equation given below [43]:

$$\varepsilon = \ln\left[1 + \frac{\Delta L}{\text{L0}}\right] = \text{-ln}(\cos\alpha) \tag{8}$$

where ε - Strain.

ΔL - Elongation during break point (in mm)

L0 - Gauge Length (in mm)

α - Micrfibril angle (in degrees)

3. Results and discussion

3.1. Morphological analysis

Fig. 2-(a–c) shows the SEM analysis of MTBF. SEM micrograph shows the inner structure the MTBF. Fig. 2(a–b) confirms the spherical structure of both primary and secondary cell walls. The SEM (Scanning Electron Microscopy) also illustrates that these Cell walls are arranged in a honeycomb-like fashion. The microfibrils are supposed to have rough surfaces adequately along with concentric rings and sieve tubular formations [44]. The fiber cell is composed of a primary cell wall, secondary cell wall and lumen. The primary cell wall looks thin and extensible with a mean diameter of about 36.4 μm and thickness of about 0.82 μm. On the other side, the secondary cell wall is thick and robust with an estimated mean diameter of 32.013 ± 1.43 μm and thickness of about 3 μm [41]. The

cell diameter is very close to the mean diameter of *Calotropis gigantea* [13] (32 μm). SEM images reveal starch grains dispersed all around the single bark fiber. The lumen structures are shown in Fig. 2(a) where the lumen diameter is about 3 μm. The lumen diameter is comparatively less than Chrysanthemum morifolium fiber (4 μm) [45]. These structures are observed in detail in Fig. 2(b). Similar structures have been previously examined in the natural fibers of Musa paradisiaca L [10]. Fig. 2(a) shows a rough surface of the MTBF, which allows better physical interface with the polymeric matrix, resulting in improved mechanical properties. Fig. 2(d) gives the particle size variation in the specimen fiber. The Cross sectional area of the fiber is examined using SEM at magnification of 400 × respectively [9].

3.2. Zeta potential and particle size measurement

The mean value of zeta potential was found to be -24.67 ± 2.3 mV. This potential value indicated the enhanced particle behavior of its surface. Furthermore, particle size of the MTBF was characterized under a few main groups around which the particle sizes are distributed, which are listed as 1 % around 9 μm, 85 % around 15.4 μm and remaining 10.35 μm. The distribution plot for particle size measurement is shown-in Fig. 2-(d).

3.3. Physio-chemical analysis

The density (ρ_{MTF}) of the bark fiber [33] was evaluated as 1.4875 g/ cm^3 from equation (1). The results of the physio-chemical analysis revealed that MTBF was composed of 54.35 % cellulose constituents. The cellulose content in the MTBF is approximately 12 % higher than coir fiber and 21 % higher than *Chrysanthemum morifolium* [45]. High proportion of cellulose in bark determines high mechanical properties. The MTBF was found to have 10 % lignin, which is higher than the bark fibers of orange [46]. The moisture content in the MTBF was estimated as 6.2 % by using equation (2). Table 2 shows the chemical composition in wt% of the MTBF.

3.4. Structural characterizations

3.4.1. Molecular weight determination

The molecular weight of the MTBF was found between the range 37.3 and 86.04 kDa from the standard curve method by using equation (3). The molecular weight directly suggests the polysaccharide structures present in the bark samples. Variation in molecular weight affects pharmacological behavior of plant polysaccharides [36,52]. The resultant parameters of MTBF showed a unique and linear arrangement of molecules without many voids. Hence it is evident that MTBF may be suitable for polymer reinforcements.

3.5. Colorimetric and monosaccharide compositions

The phenol-sulfuric acid method showed the percentage of carbohydrates to be 78 %. Carbazole method revealed the presence of uronic acids to be 4 %. Furthermore, Coomassie blue protein technique revealed the protein concentrations as 1.3 %. Sulfates were detected to be 3.4 % by barium chloride–gelatin method. The hydroxylamine colorimeter test showed the presence of O-acetyl polysaccharides as 4.6 %. The composition of a marginal amount of enough sulfate- and O-acetyl polysaccharides in MTBFs enhances anti-oxidant and allied pharmaceutical properties [36]. The monosaccharide composition of the MTBF showed the presence of polysaccharides with minute content of uronic acids (~4 %) along with acetyl- and -aldehyde groups (~4.6 %). The presence of these compositions contributes to surface absorption and chemical bonding in polymer reinforcements [36]. The experimental readings are shown in Table 2.

3.6. Methylation

The method showed various linkages of PMAA (partially methylated alditol acetates) of glucosidic acetates (sugar residues). Table 2 shows the temperature change rate for methylation analysis. The MTBF is rich in sugar residues like Man, Ara, Gal, and Rha. The glycosidic residues are found in the molar ratio of 21.8: 12.7: 35.6: 20.4 (Man-Ara-Gal-Rha). The glycosidic linkage ratio reveals a strong intermolecular bonding between fiber particles. This also ensures strong surface absorption property of the MTBF [36].

Table 2
Chemical composition (in wt%).

Fiber	Cellulose	Hemi-Cellulose	Lignin	Wax	Ash	Moisture	References
MT bark	54.35	16.63	10.87	2.35	9.60	6.2	Present Work
Putranjiva roxburghii	46.56	19.34	23.58	1.82	1.82	6.24	[47]
Althaea officinalis L.	44.6	13.5	2.7	–	2.3	–	[48]
Albizia amara bark	64.54	9.41	15.61	0.56	4.1	9.34	[49]
Prosopis juliflora bark	61.65	16.14	17.11	0.61	5.2	9.48	[42]
Ficus Racemosa bark	72.36	11.21	10.45	0.25	6.59	6.13	[50]
Carica papaya bark	58.71	11.8	14.26	0.81	4.7	9.73	[51]

3.7. Smith degradations

The composition results obtained through Smith degradations are shown. Table 3 shows Smith degradation values that change with temperature at a specified rate.

The results show a cohesive reaction of TMSA derivatives with the fiber surface. The experiment also reveals that the covalent bonds on the fiber surface are hard to break, and once reinforced, they are hard enough to react chemically.

3.8. XRD analysis

Fig. 3 shows the XRD spectrum of the MTBF sample. The primary crystalline peak at $2\theta^{\circ} = 21.97^{\circ}$ resembles the cellulose crystallographic plane. The lower-intensity peak at $2\theta^{\circ} = 14.76^{\circ}$ resembles the amorphous plane in the fiber, showing a large amount of chemical compositions including amorphous cellulose, hemicellulose, and lignin [43]. The peak at 29.49° indicates the presence of a lattice spacing crystalline structure in the fiber [17]. Earlier researches has also confirmed that this peak corresponds to (0 0 2) diffraction of cellulose and mineral elements. Similar peak has also been identified in various other works such as Modification Methods of Wheat Straw Fibers [53], Cellulose nano-fibrils from Wheat straw [54], characterization of radio frequency assisted with flax fibers [55], Alkali treated Bamboo fibers [56] and pretreatment and hydrolysis on Corn straw [57]. Crystallinity index value of the MTBF is calculated as 51 % by Segal equation (equation (4)). The CI value of the MTBF is higher than that of the *Thespesia populnea* (48 %) [7], *Cissus vitiginea* (30.5 %), *Prosopis juliflora* (46 %) [58] barks, *Hierochloe odorata* fiber (32.9 %) [59] and lower than that of *C. morifolium* (65.18 %) [45] and mulberry barks (58.8 %) [58]. The low crystallite values confirm that the surface can control high chemical reactiveness and water absorption of the experimental sample. The CS of the MTBF was assessed as 3.086 nm using the Scherer formula (equation (5)), which is greater than that of *Ferula communis* (1.6 nm) and *Althaea officinalis* (2.4 nm) and lower than that of *Aloe vera* (5.72 nm) and *Thespesia populnea* (3.576 nm) [58].

3.9. FTIR analysis

Fig. 4 and Table 4 shows a clear picture of the FTIR spectra of the MTBF. The peaks at 3906 and 518 cm^{-1} confirm the presence of O–H bonding of hydrogen, water, and hydrogen groups. The peak at 3530 cm^{-1} is attributed to the C–O stretching. Similar values are earlier reported in *Prospis juliflora* bark [42]. The peaks at 2922 and 873 cm^{-1} are associated with high C–H bonds. The C–H wagging is endorsed by the peak at 1456 cm^{-1}. Similar values are earlier found for *Dichrostachys cinerea* bark [60]. The C–O stretching is evident at 1267 cm^{-1} and 1194 $^{-}cm^{-1}$. The C═C aromatic stretches are noted at both low-energy peaks at 1508 cm^{-1} and 1421 cm^{-1}. Similar values are earlier noted for *Ceiba pentandra* bark [61]. The peak at 3319 cm^{-1} is due to the influence of cellulose constituents. The peak at 1653 cm^{-1} is attributed to the free ester carboxyl group [9].

3.10. Thermogravimetric analysis

Table 5 compares the values of thermal analysis of MTBF with previous readings, and thermogravimetric analysis (TGA) and DTG graphs are shown in Fig. 5-(a) and (b). The DTG curve shows the removal of water and chemical compositions, indicating better reinforcement for substantial stability at high temperatures. The DTG curve shows the temperature-dependent degradation of fiber composition in terms of weight percentage. The initial weight loss of 4 % occurs at around 62 °C. This primary weight-loss peak, occurring at atmospheric conditions, is mainly due to the degradation of hydrogen, moisture, and carboxyl groups present in MT bark. At 34 °C, tannins and hemicellulose degrade. At 182 °C, glycosidic bond breakage and depolymerization of lignin are observed [10]. The major weight degradation of the fiber occurs between 234 °C and 350 °C, where all the glycosidic bonds, lignin, and hemicellulose thermally depolymerize. The curve shows distinct peak overshoots corresponding to the degradation of cellulose and non-cellulose components. The first peak at around 180 °C shows depolymerization of hemicellulose. Similarly, degradation of cellulose is seen at around 450 °C.

The TGA–DTG curves of MTBF are similar to those of *Coccinia grandis* and *Aramid* [33]. At around 320 °C, fiber completely loses its thermal withstanding capability and complete degradation occurs. In comparison with earlier records, the thermal analysis on the MTBF revealed it to be thermally stable up to 240 °*C*, which is nearer to linen fibers [65] and Nendran Banana Peduncle plants [66]. Similar primary weight-loss peaks for DTG and TGA are earlier reported for spruce bark [39], *Centaurea solstitialis* [67], and *C. pentandra* barks [61]. After 347 °C, depolymerization of ∝-cellulose is noted. Char content is seen as residual degradation at around 500 °C.

Fig. 5(c) shows Broido's plot for MTBF. KE is found to be 96.867 kJ/mol by Broido's equation (6) [40]. The obtained value is lesser

Table 3
Structural characterizations.

Rate(°C/min)	Monosaccharide Composition Temperature(°C)	Methylation Temperature(°C)	Smith degradation Temperature(°C)
0	170	135	98–100
5	215–225	235–260	140
10	230–290	260–290	150–175

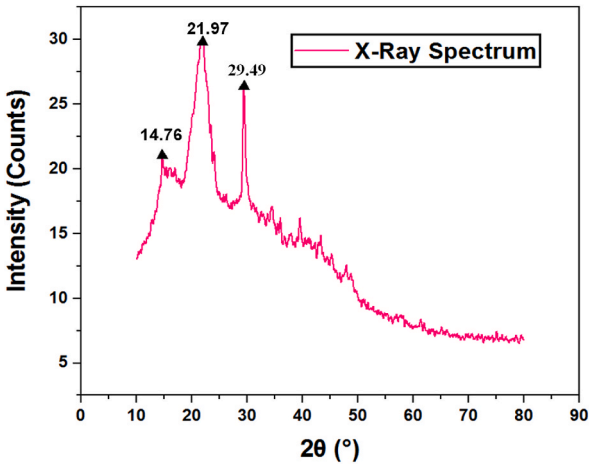

Fig. 3. XRD analysis.

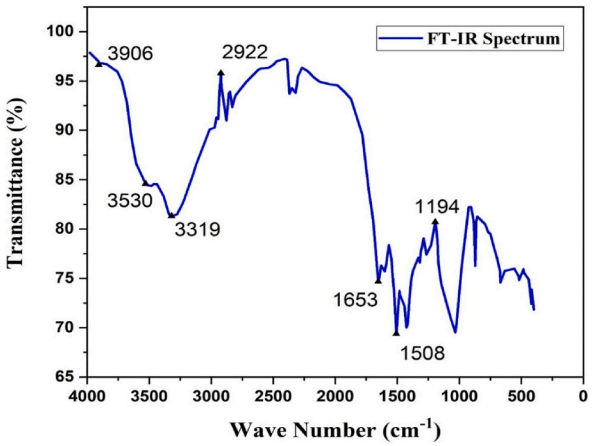

Fig. 4. FTIR graph of MTBF

Table 4
FTIR Peak positions and its allocations.

Peak Positions in cm^{-1}	Allocations
3906	O–H bonding of hydrogen
3530	C–O stretching
3319	influence of cellulose constituents
2922	high C–H bonds
1653	free ester carboxyl group
1508	C═C aromatic stretches
1456	C–H wagging
1267 & 1194	C–O stretching

Table 5
Comparison of thermal analysis.

Fiber	$T_g(^\circ C)$	$T_d(^\circ C)$	References
MTBF	240	330	This work
Ferula bark	200	313.5	[62]
Bino	220	338.7	[41]
Arundo d. bark	275	320	[63]
Prosopis juliflora bark	217	331.1	[42]
Thespesia lampas	230	270–360	[64]

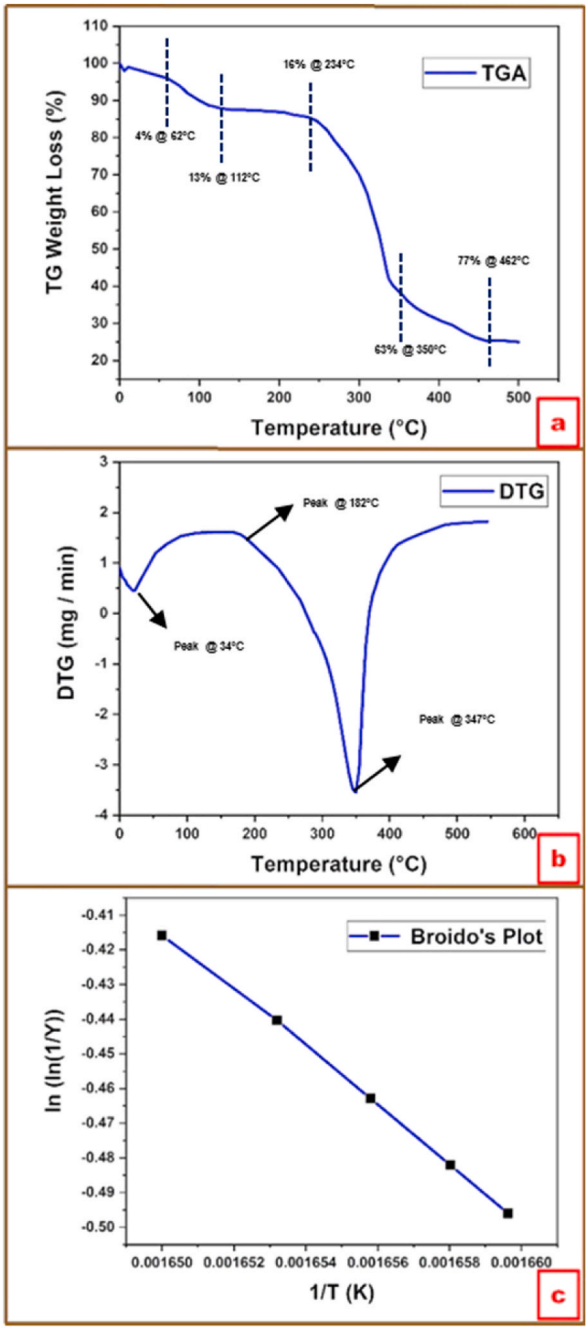

Fig. 5. a)TGA, b)DTG, c)Broido's plot.

Table 6
Tensile characteristics of MTBF.

Gauge length (mm)	Maximum tensile strength (MPa)	Breakdown strain (%)	Young 's modulus (GPa)	Cross Sectional Area (mm^2)
10	460.34	15.6	27.85	0.0134
20	655.87	7.8	65.12	0.0124
30	736.27	6.0	71.15	0.0093
50	746.77	5.90	75.69	0.0094
70	557.65	5.7	59.64	0.0095

than that of *Ficus religiosa* tree (68.02 kJ/mol) [68]. The KE value within the range 60–170 kJ/mol shows stability over a wide range of temperatures. This shows the possibility of composite polymerization and thermal stability over high temperature.

3.11. Tensile characteristics

The tensile strength of MT bark was measured for 50 mm gauge length as per the accordance of ASTM Standard D 3379–2002, which was found to be 746.77 MPa. It was higher than that of *Derris scandens* (633.87 MPa) [69] and hemp bark fibers (690 MPa) [70]. Tensile properties of MT bark specimen obtained from the experiment in variation to gauge length are shown in Table 6. By using equation (7), the interfacial shear strength (τ_d) of the MTBF was calculated to be 9.87 MPa, which confirmed that the MTBF possesses an isotropic high stiffness as discussed in Ref. [42]. The tensile strength of MTBF was calculated to be 746.77 MPa at 6.0 % strain rate. The Young's modulus value was predicted to be 75.7 GPa with the help of equation (8) where α (microfibril angle) $= 12.62^{\circ} \pm 0.35^{\circ}$. Comparison on Microfibril angle of other bark fibers with the derived microfibril angle of MTBF has been listed in Table 7 respectively. The microfibril angle of MTBF is calculated using equation (8). Young's value of MT was higher than that of banana fiber (67 GPa) [71] and *Acacia leucophloea* bark (69.6 GPa) [70]. Tensile parameters along with mechanical characteristics of MTBF are listed in Table 8.

4. Conclusion

The study focuses on finding an eco-friendly, novel bark fiber in an attempt to substitute synthetic fibers with polymer composites. The microfibrils extracted from the MTBF were examined for their morphological, physio-chemical, mechanical, and structural properties.

- ❖ The structural characterization has also indicated the fiber's potential for strong-surface interactions. The enhanced behavior of MTBF in structural characterization provides a scope for the fiber to be used as a reinforcing substrate in dielectric and bio-composite applications.
- ❖ The mechanical properties of the MT bark specimen are measured by tensile test and its results were analyzed using ASTM standards. The MTBF showed a potential for greater strain and shearing strength.
- ❖ This shows that MTBF micro composite has a wide scope for use in the fields of automobile, textile, and packaging industries. Therefore, it can substitute existing materials as a bio composite derived from the bark of the Indian mulberry plant in various polymer applications owing to its behavior.

In conclusion, the results of physiochemical, tensile, and thermal analyses showed that MTBF has optimal characteristics compared to various other natural cellulosic bark fibers. Future research on MTBF can be extended to develop a novel polymer-reinforced composite for the development of eco-friendly agro-domestic and thermoplastic dielectric composites, as the material would possess huge potential for dielectric behavior.

Ethical approval

Not Applicable.

Funding

Not Applicable.

Data availability statement

No data was used for the research described in the article.

CRediT authorship contribution statement

Gurukarthik Babu Balachandran: Conceptualization, Data curation, Formal analysis, Funding acquisition, Investigation, Methodology, Project administration, Resources, Software, Supervision, Validation, Visualization, Writing – original draft, Writing – review & editing. **P. Narayanasamy:** Conceptualization, Data curation, Formal analysis, Funding acquisition, Investigation, Methodology, Project administration, Resources, Software, Supervision, Validation, Visualization, Writing – original draft, Writing – review & editing. **Anandha Balaji Alexander:** Conceptualization, Data curation, Formal analysis, Funding acquisition, Investigation, Methodology, Project administration, Resources, Software, Supervision, Validation, Visualization, Writing – original draft, Writing – review & editing. **Prince Winston David:** Conceptualization, Data curation, Formal analysis, Funding acquisition, Investigation, Methodology, Project administration, Resources, Software, Supervision, Validation, Visualization, Writing – original draft, Writing – review & editing. **Rajesh Kannan Mariappan:** Conceptualization, Data curation, Formal analysis, Funding acquisition, Investigation, Methodology, Project administration, Resources, Software, Supervision, Validation, Visualization, Writing – original draft, Writing – review & editing. **Muthu Eshwaran Ramachandran:** Conceptualization, Data curation, Formal analysis, Funding acquisition, Investigation, Methodology, Project administration, Resources, Software, Supervision, Validation, Visualization, Writing – original

Table 7
Comparison of Microfibril angle.

Bark Fibers	Microfibril angle in °
Morinda tinctoria	12.62 ± 0.35°
Flax Fiber	5°
Hemp Fiber	6.2°
Cochlospermum orinocense	7.32°
Jute Fiber	8.1°
Epipremnum aureum	9.46–12.18°
Acacia leucophloea	9.5–16.56°
Prosopis juliflora	10.64° ± 0.45°
Banana Fiber	11–12°
Piliostigma racemosa	18.9°

Table 8
Comparison of tensile properties.

Fiber	Mechanical behavior			
	Tensile strength (MPa)	Young's modulus (GPa)	Strain to failure (%)	References
MTBF	746.77	75.7	6	This work
Coccinia grandis bark	424–775	70	5.6–16	[33]
Acacia leucophloea bark	1608	69.6	4.24	[70]
Cissus vitiginea bark	315.24	6.05	8.96	[58]
Thespesia bark	573	61.2	0.79	[64]

draft, Writing – review & editing. **Suyambulingam Indran:** Conceptualization, Data curation, Formal analysis, Funding acquisition, Investigation, Methodology, Project administration, Resources, Software, Supervision, Validation, Visualization, Writing – original draft, Writing – review & editing. **Sanjay Mavinkere Rangappa:** Conceptualization, Data curation, Formal analysis, Funding acquisition, Investigation, Methodology, Project administration, Resources, Software, Supervision, Validation, Visualization, Writing – original draft, Writing – review & editing. **Suchart Siengchin:** Conceptualization, Data curation, Formal analysis, Funding acquisition, Investigation, Methodology, Project administration, Resources, Software, Supervision, Validation, Visualization, Writing – original draft, Writing – review & editing.

Declaration of competing interest

The authors declare that they have no known competing financial interests or personal relationships that could have appeared to influence the work reported in this paper.

Acknowledgment

This research was funded by King Mongkut's University of Technology North Bangkok with Contract no. KMUTNB-67-KNOW-26.

References

[1] M.R. Sanjay, P. Madhu, M. Jawaid, P. Senthamaraikannan, S. Senthil, S. Pradeep, Characterization and properties of natural fiber polymer composites: a comprehensive review, J. Clean. Prod. 172 (2018) 566–581, https://doi.org/10.1016/j.jclepro.2017.10.101.
[2] B. Gurukarthik Babu, D. Princewinston, V.C. Padmanaban, G.A. Lathief Sherief, M. Kiruba Sankar, P.V. Aravind Bhaskar, Optimization studies on improving the dielectric properties of alkali treated fibers from phaseolus vulgaris reinforced polyester composites by central composite design, J. Nat. Fibers 00 (00) (2019) 1–11, https://doi.org/10.1080/15440478.2019.1697985.
[3] B. Gurukarthik Babu, D. Prince Winston, P.V. Aravind Bhaskar, R. Baskaran, P. Narayanasamy, Exploration of electrical, thermal, and mechanical properties of Phaseolus vulgaris fiber/unsaturated polyester resin composite filled with nano–SiO2, J. Nat. Fibers 00 (00) (2020) 1–17, https://doi.org/10.1080/15440478.2020.1724231.
[4] A. Arul Marcel Moshi, D. Ravindran, S.R. Sundara Bharathi, S. Indran, G. Suganya Priyadharshini, Characterization of surface-modified natural cellulosic fiber extracted from the root of Ficus religiosa tree, Int. J. Biol. Macromol. 156 (2020) 997–1006, https://doi.org/10.1016/j.ijbiomac.2020.04.117.
[5] S. Hossain, M.A. Jalil, T. Islam, M.M. Rahman, A low-density cellulose rich new natural fiber extracted from the bark of jack tree branches and its characterizations, Heliyon 8 (no. 11) (2022), https://doi.org/10.1016/j.heliyon.2022.e11667.
[6] D.T. Ebissa, T. Tesfaye, D. Worku, D. Wood, Characterization and optimization of the properties of untreated high land bamboo fibres, Heliyon 8 (8) (2022), e09856, https://doi.org/10.1016/j.heliyon.2022.e09856.
[7] M. Kathirselvam, A. Kumaravel, V.P. Arthanarieswaran, S.S. Saravanakumar, Characterization of cellulose fibers in Thespesia populnea barks: influence of alkali treatment, Carbohydr. Polym. 217 (2019) 178–189, https://doi.org/10.1016/j.carbpol.2019.04.063.
[8] R. Prithivirajan, et al., Characterization of cellulosic fibers from Morus alba L. stem, J. Nat. Fibers 16 (4) (2019) 503–511, https://doi.org/10.1080/15440478.2018.1426079.
[9] R.S. Kumar, et al., A new natural cellulosic pigeon pea (Cajanus cajan) pod fiber characterization for bio-degradable polymeric composites, J. Nat. Fibers 0 (0) (2019) 1–11, https://doi.org/10.1080/15440478.2019.1689887.
[10] R. Prithivirajan, et al., Characterization of Musa paradisiaca L. Cellulosic natural fibers from agro-discarded blossom petal waste, J. Nat. Fibers 17 (11) (2020) 1640–1653, https://doi.org/10.1080/15440478.2019.1588826.

[11] B. Gurukarthik Babu, et al., Study on characterization and physicochemical properties of new natural fiber from Phaseolus vulgaris, J. Nat. Fibers 16 (7) (2019) 1035–1042, https://doi.org/10.1080/15440478.2018.1448318.

[12] J.S. Binoj, R. Edwin Raj, B.S.S. Daniel, Comprehensive characterization of industrially discarded fruit fiber, Tamarindus indica L. as a potential eco-friendly bio-reinforcement for polymer composite, J. Clean. Prod. 142 (2017) 1321–1331, https://doi.org/10.1016/j.jclepro.2016.09.179.

[13] P. Narayanasamy, et al., Characterization of a novel natural cellulosic fiber from Calotropis gigantea fruit bunch for ecofriendly polymer composites, Int. J. Biol. Macromol. 150 (2020) 793–801, https://doi.org/10.1016/j.ijbiomac.2020.02.134.

[14] P. Balasundar, et al., Physico-chemical study of pistachio (Pistacia vera) nutshell particles as a bio-filler for eco-friendly composites, Mater. Res. Express 6 (10) (2019), https://doi.org/10.1088/2053-1591/ab3b9b.

[15] S.N. R. I, R. T, Characterization of untreated and alkali treated new cellulosic fiber from an Areca palm leaf stalk as potential reinforcement in polymer composites, Carbohydr. Polym. 195 (2018) 566–575, https://doi.org/10.1016/j.carbpol.2018.04.127.

[16] T. Ganapathy, R. Sathiskumar, P. Senthamaraikannan, S.S. Saravanakumar, A. Khan, Characterization of raw and alkali treated new natural cellulosic fibres extracted from the aerial roots of banyan tree, Int. J. Biol. Macromol. 138 (2019) 573–581, https://doi.org/10.1016/j.ijbiomac.2019.07.136.

[17] A. Kar, D. Saikia, Characterization of new natural cellulosic fiber from Calamus tenuis (Jati Bet) cane as a potential reinforcement for polymer composites, Heliyon 9 (6) (2023), e16491, https://doi.org/10.1016/j.heliyon.2023.e16491.

[18] D. Bhakta, R. Siva, Amelioration of oxidative stress in bio-membranes and macromolecules by non-toxic dye from Morinda tinctoria (Roxb.) roots, Food Chem. Toxicol. 50 (6) (2012) 2062–2069, https://doi.org/10.1016/j.fct.2012.03.045.

[19] A. Amalraj, A. Pius, Removal of fluoride from drinking water using aluminum hydroxide coated activated carbon prepared from bark of Morinda tinctoria, Appl. Water Sci. (2016), https://doi.org/10.1007/s13201-016-0479-z.

[20] K. Krishnaveni, J. Ravichandran, Influence of aqueous extract of leaves of Morinda tinctoria on copper corrosion in HCl medium, J. Electroanal. Chem. 735 (2014) 24–31, https://doi.org/10.1016/j.jelechem.2014.09.032.

[21] K. Krishnaveni, J. Ravichandran, Effect of aqueous extract of leaves of Morinda tinctoria on corrosion inhibition of aluminium surface in HCl medium, Trans. Nonferrous Metals Soc. China 24 (8) (2014) 2704–2712, https://doi.org/10.1016/S1003-6326(14)63401-4.

[22] K. Deepti, P. Umadevi, G. Vijayalakshmi, B.V. polarao, Antimicrobial activity and phytochemical analysis of Morinda tinctoria roxb. Leaf extracts, Asian Pac. J. Trop. Biomed. 2 (Supplement) (2012) S1440–S1442, https://doi.org/10.1016/S2221-1691(12)60433-X, 3.

[23] N. Kannan, M. Manokari, M.S. Shekhawat, Enhanced production of anthraquinones and phenolic compounds using chitosan from the adventitious roots of Morinda coreia Buck. and Ham, Ind. Crops Prod. 148 (2020), 112321, https://doi.org/10.1016/j.indcrop.2020.112321.

[24] K.R. Kumar, N. Nattuthurai, P. Gopinath, T. Mariappan, Synthesis of eco-friendly silver nanoparticles from Morinda tinctoria leaf extract and its larvicidal activity against Culex quinquefasciatus, Parasitol. Res. 114 (2) (2015) 411–417, https://doi.org/10.1007/s00436-014-4198-9.

[25] M. Subramanian, S. Balakrishnan, S.K. Chinnaiyan, V.K. Sekar, A.N. Chandu, Hepatoprotective effect of leaves of Morinda tinctoria Roxb. against paracetamol induced liver damage in rats, Drug Invent. Today 5 (3) (2013) 223–228, https://doi.org/10.1016/j.dit.2013.06.008.

[26] A. Khouaja, A. Koubaa, H. Ben Daly, Dielectric properties and thermal stability of cellulose high-density polyethylene bio-based composites, Ind. Crops Prod. 171 (2021), 113928, https://doi.org/10.1016/j.indcrop.2021.113928.

[27] J. Dou, A. Karakoç, L.-S. Johansson, S. Hietala, D. Evtyugin, T. Vuorinen, Mild alkaline separation of fiber bundles from eucalyptus bark and their composites with cellulose acetate butyrate, Ind. Crops Prod. 165 (2021), 113436, https://doi.org/10.1016/j.indcrop.2021.113436.

[28] A.A. Salema, Y.K. Yeow, K. Ishaque, F.N. Ani, M.T. Afzal, A. Hassan, Dielectric properties and microwave heating of oil palm biomass and biochar, Ind. Crops Prod. 50 (2013) 366–374, https://doi.org/10.1016/j.indcrop.2013.08.007.

[29] B.G. Babu, et al., Investigation on the physicochemical and mechanical properties of novel alkali-treated Phaseolus vulgaris fibers, J. Nat. Fibers 00 (00) (2020) 1–12, https://doi.org/10.1080/15440478.2020.1761930.

[30] X. Miao, J. Lin, F. Tian, X. Li, F. Bian, J. Wang, Cellulose nanofibrils extracted from the byproduct of cotton plant, Carbohydr. Polym. 136 (2016) 841–850, https://doi.org/10.1016/j.carbpol.2015.09.056.

[31] Y. Huang, S.S. Nair, H. Chen, B. Fei, N. Yan, Q. Feng, Lignin-rich nanocellulose fibrils isolated from parenchyma cells and fiber cells of western red cedar bark, ACS Sustain. Chem. Eng. 7 (18) (2019) 15607–15616, https://doi.org/10.1021/acssuschemeng.9b03634.

[32] J. Paulo, et al., Extraction and characterization of nanocellulose structures from raw cotton linter, Carbohydr. Polym. 91 (1) (2013) 229–235, https://doi.org/10.1016/j.carbpol.2012.08.010.

[33] S.G. Jebadurai, R.E. Raj, V.S. Sreenivasan, J.S. Binoj, Comprehensive characterization of natural cellulosic fi ber from Coccinia grandis stem, Carbohydr. Polym. 207 (2019) 675–683, https://doi.org/10.1016/j.carbpol.2018.12.027. December 2018.

[34] K. Kürschner, et al., Cellulose und Cellulosederivate, Z. für Anal. Chem. 92 (3–4) (1933) 145–154.

[35] I. A. Pearl and Others, "The Chemistry of lignin.,", Chem. lignin., 1967.

[36] Y. Xia, T. Wang, S. Yu, J. Liang, H. Kuang, Structural characteristics and hepatoprotective potential of Aralia elata root bark polysaccharides and their e ff ects on SCFAs produced by intestinal fl ora metabolism, Carbohydr. Polym. 207 (December 2018) (2019) 256–265, https://doi.org/10.1016/j.carbpol.2018.11.097.

[37] C.M. Pagliosa, et al., Characterization of the bark from residues from mate tree harvesting (Ilex paraguariensis St. Hil.), Ind. Crops Prod. 32 (3) (2010) 428–433, https://doi.org/10.1016/j.indcrop.2010.06.010.

[38] C. Wijaya, et al., Isolation and characterization of starch from Limnophila aromatica, Heliyon 5 (5) (2019), e01622, https://doi.org/10.1016/j.heliyon.2019.e01622.

[39] M. Le Normand, R. Moriana, M. Ek, Isolation and characterization of cellulose nanocrystals from spruce bark in a biorefinery perspective, Carbohydr. Polym. 111 (2014) 979–987, https://doi.org/10.1016/j.carbpol.2014.04.092.

[40] N. Reddy, Y. Yang, Structure and properties of high quality natural cellulose fibers from cornstalks, Polymer (Guildf). 46 (15) (2005) 5494–5500, https://doi.org/10.1016/j.polymer.2005.04.073.

[41] Z. Belouadah, A. Ati, M. Rokbi, Characterization of new natural cellulosic fiber from Lygeum spartum L, Carbohydr. Polym. 134 (2015) 429–437, https://doi.org/10.1016/j.carbpol.2015.08.024.

[42] S.S. Saravanakumar, A. Kumaravel, T. Nagarajan, P. Sudhakar, R. Baskaran, Characterization of a novel natural cellulosic fiber from Prosopis juliflora bark, Carbohydr. Polym. 92 (2) (2013) 1928–1933, https://doi.org/10.1016/j.carbpol.2012.11.064.

[43] M.V. Maheshwaran, N.R.J. Hyness, P. Senthamaraikannan, S.S. Saravanakumar, M.R. Sanjay, Characterization of natural cellulosic fiber from Epipremnum aureum stem, J. Nat. Fibers 15 (6) (2018) 789–798, https://doi.org/10.1080/15440478.2017.1364205.

[44] I. Baptista, I. Miranda, T. Quilhó, J. Gominho, H. Pereira, Characterisation and fractioning of Tectona grandis bark in view of its valorisation as a biorefinery raw-material, Ind. Crops Prod. 50 (2013) 166–175, https://doi.org/10.1016/j.indcrop.2013.07.004.

[45] R. Dalmis, G.B. Kilic, Y. Seki, S. Koktas, O.Y. Keskin, Characterization of a novel natural cellulosic fiber extracted from the stem of Chrysanthemum morifolium, Cellulose 27 (15) (2020) 8621–8634, https://doi.org/10.1007/s10570-020-03385-2.

[46] E. Espinosa, R.I. Arrebola, I. Bascón-Villegas, M. Sánchez-Gutiérrez, J. Domínguez-Robles, A. Rodríguez, Industrial application of orange tree nanocellulose as papermaking reinforcement agent, Cellulose 27 (18) (2020) 10781–10797, https://doi.org/10.1007/s10570-020-03353-w.

[47] K.M. Muthukrishnan, G. Selvakumar, P. Narayanasamy, P. Ravindran, Characterization of raw and alkali treated cellulosic filler isolated from putranjiva roxburghii W. Seed shell roadside vegetative residues, J. Nat. Fibers 19 (16) (2022) 14287–14298, https://doi.org/10.1080/15440478.2022.2061670.

[48] M. Kathirselvam, A. Kumaravel, V.P. Arthanarieswaran, S.S. Saravanakumar, Isolation and characterization of cellulose fibers from Thespesia populnea barks: a study on physicochemical and structural properties, Int. J. Biol. Macromol. 129 (2019) 396–406, https://doi.org/10.1016/j.ijbiomac.2019.02.044.

[49] P. Senthamaraikannan, M.R. Sanjay, K.S. Bhat, N.H. Padmaraj, M. Jawaid, Characterization of natural cellulosic fiber from bark of Albizia amara, J. Nat. Fibers 00 (00) (2018) 1–8, https://doi.org/10.1080/15440478.2018.1453432.

[50] P. Manimaran, S.P. Saravanan, M. Prithiviraj, Investigation of Physico Chemical Properties and Characterization of New Natural Cellulosic Fibers from the Bark of Ficus Racemosa Investigation of Physico Chemical Properties and Characterization of New Natural Cellulosic Fibers from the Bark of Ficus Ra, 2019, https://doi.org/10.1080/15440478.2019.1621233, 0478.

[51] A.S. Kumaar, A. Senthilkumar, T. Sornakumar, S.S. Saravanakumar, V.P. Arthanariesewaran, Physicochemical properties of new cellulosic fiber extracted from Carica papaya bark Physicochemical properties of new cellulosic fiber extracted from, J. Nat. Fibers 00 (00) (2017) 1–10, https://doi.org/10.1080/15440478.2017.1410514.
[52] D. Sandoval-Rivas, E. Moczko, D. V Morales, M.I. Hepp, Evaluation and characterization of a new method of extracting bark wax from Pinus radiata D. Don, Ind. Crops Prod. 174 (2021), 114161, https://doi.org/10.1016/j.indcrop.2021.114161.
[53] D. Jiang, P. An, S. Cui, S. Sun, J. Zhang, T. Tuo, Effect of modification methods of wheat straw fibers on water absorbency and mechanical properties of wheat straw fiber cement-based composites, Adv. Mater. Sci. Eng. 2020 (2020), https://doi.org/10.1155/2020/5031025.
[54] A. Kaushik, M. Singh, G. Verma, Green nanocomposites based on thermoplastic starch and steam exploded cellulose nanofibrils from wheat straw, Carbohydr. Polym. 82 (2) (2010) 337–345, https://doi.org/10.1016/j.carbpol.2010.04.063.
[55] P. Ruan, J. Du, Y. Gariepy, V. Raghavan, Characterization of radio frequency assisted water retting and flax fibers obtained, Ind. Crops Prod. 69 (2015) 228–237, https://doi.org/10.1016/j.indcrop.2015.02.009.
[56] H. Chen, J. Wu, J. Shi, W. Zhang, H. Wang, Effect of alkali treatment on microstructure and thermal stability of parenchyma cell compared with bamboo fiber, Ind. Crops Prod. 164 (November) (2020) 2021, https://doi.org/10.1016/j.indcrop.2021.113380.
[57] P. Wang, et al., Effect of physicochemical pretreatments plus enzymatic hydrolysis on the composition and morphologic structure of corn straw, Renew. Energy 138 (2019) 502–508, https://doi.org/10.1016/j.renene.2019.01.118.
[58] S. Chakravarthy K, M. Madhu S, J.S. Naga Raju, J. Shariff Md, Characterization of novel natural cellulosic fiber extracted from the stem of Cissus vitiginea plant, Int. J. Biol. Macromol. 161 (2020) 1358–1370, https://doi.org/10.1016/j.ijbiomac.2020.07.230.
[59] R. Dalmis, S. Köktaş, Y. Seki, A.Ç. Kılınç, Characterization of a new natural cellulose based fiber from Hierochloe Odarata, Cellulose 27 (1) (2020) 127–139, https://doi.org/10.1007/s10570-019-02779-1.
[60] P.G. Baskaran, et al., Characterization of new natural cellulosic fiber from the bark of Dichrostachys cinerea characterization of new natural cellulosic fiber from the bark of, J. Nat. Fibers 00 (00) (2017) 1–7, https://doi.org/10.1080/15440478.2017.1304314.
[61] R. Kumar, N.R.J. Hynes, P. Senthamaraikannan, M.R. Sanjay, N.R.J. Hynes, P. Senthamaraikannan, Physicochemical and thermal properties of Ceiba pentandra bark fiber physicochemical and thermal properties of Ceiba pentandra bark, J. Nat. Fibers 00 (00) (2017) 1–8, https://doi.org/10.1080/15440478.2017.1369208.
[62] Y. Seki, M. Sarikanat, K. Sever, C. Durmuşkahya, Extraction and properties of Ferula communis (chakshir) fibers as novel reinforcement for composites materials, Compos. Part B Eng. 44 (1) (2013) 517–523, https://doi.org/10.1016/j.compositesb.2012.03.013.
[63] V. Fiore, T. Scalici, A. Valenza, Characterization of a new natural fiber from Arundo donax L. as potential reinforcement of polymer composites, Carbohydr. Polym. 106 (2014) 77–83, https://doi.org/10.1016/j.carbpol.2014.02.016.
[64] K.O. Reddy, B. Ashok, K.R.N. Reddy, Y.E. Feng, J. Zhang, A.V. Rajulu, Extraction and characterization of novel lignocellulosic fibers from Thespesia lampas plant, Int. J. Polym. Anal. Char. 19 (1) (2014) 48–61, https://doi.org/10.1080/1023666X.2014.854520.
[65] H. Li, Z. Li, Y. Liu, M. Li, Advantages of Scutellaria baicalensis extracts over just baicalin in the ultrasonically assisted multi-functional treatment of linen fabrics, Cellulose 27 (8) (2020) 4831–4846, https://doi.org/10.1007/s10570-020-03109-6.
[66] P. Manimaran, G.P. Pillai, V. Vignesh, M. Prithiviraj, Characterization of natural cellulosic fibers from Nendran Banana Peduncle plants, Int. J. Biol. Macromol. 162 (2020) 1807–1815, https://doi.org/10.1016/j.ijbiomac.2020.08.111.
[67] O.Y. Keskin, R. Dalmis, G. Balci Kilic, Y. Seki, S. Koktas, Extraction and characterization of cellulosic fiber from Centaurea solstitialis for composites, Cellulose 27 (17) (2020) 9963–9974, https://doi.org/10.1007/s10570-020-03498-8.
[68] A.A.M. Moshi, D. Ravindran, S.R.S. Bharathi, S. Indran, S.S. Saravanakumar, Y. Liu, Characterization of a new cellulosic natural fiber extracted from the root of Ficus religiosa tree, Int. J. Biol. Macromol. 142 (2020) 212–221, https://doi.org/10.1016/j.ijbiomac.2019.09.094.
[69] I.P. C, S. R, Characterization of a new natural cellulosic fiber extracted from Derris scandens stem, Int. J. Biol. Macromol. 165 (2020) 2303–2313, https://doi.org/10.1016/j.ijbiomac.2020.10.086.
[70] V.P. Arthanarieswaran, A. Kumaravel, S.S. Saravanakumar, Characterization of new natural cellulosic fiber from Acacia leucophloea bark, Int. J. Polym. Anal. Char. 20 (4) (2015) 367–376, https://doi.org/10.1080/1023666X.2015.1018737.
[71] K.Z.M.A. Motaleb, R. Al Mizan, R. Milašius, Development and characterization of eco-sustainable banana fiber nonwoven material: surface treatment, water absorbency and mechanical properties, Cellulose 27 (14) (2020) 7889–7900, https://doi.org/10.1007/s10570-020-03343-y.